



Estimating multi-frequency satellite phase biases of BeiDou using maximal decorrelated linear ambiguity combinations

Gen Liu¹ · Xiaohong Zhang^{1,2,3} · Pan Li^{1,4}

Received: 3 September 2018 / Accepted: 18 February 2019 / Published online: 25 February 2019
© Springer-Verlag GmbH Germany, part of Springer Nature 2019

Abstract

Improving ambiguity resolution (AR) in multi-frequency undifferenced and uncombined precise point positioning (PPP) benefits from accurate uncalibrated phase delays (UPD), which are often estimated from linear combinations of float ambiguities. The traditional linear ambiguity combinations for estimating these UPDs in case of triple-frequency observations are typically extra-wide-lane, wide-lane, and $L1$ combinations. We proposed the method for estimating UPDs from triple-frequency ambiguities using maximal decorrelated linear ambiguity combinations obtained by the least-squares ambiguity decorrelation adjustment Z -transformation. To validate the quality and availability of estimating UPDs for the BeiDou navigation satellite system, based on maximal decorrelated linear ambiguity combinations, tests using observations from stations of the Crustal Movement Observation Network of China and the Asia-Pacific Reference Frame project are performed using undifferenced and uncombined PPP-AR. The results show the internal precision of combined satellite UPDs estimated from the maximal decorrelated linear ambiguity combinations is better than that estimated from traditional combinations in terms of temporal stability and RMS of posteriori residuals. Furthermore, the statistical results also demonstrated that triple-frequency PPP-AR using the improved UPDs reduces the average convergence time by 8.9 and 12.3% in horizontal and vertical directions, and also improves the positioning accuracy for 3 h of observations by 11.1, 9.1 and 8.3% in the east, north and up directions, respectively, compared with triple-frequency PPP-AR using the UPDs derived from the traditional combinations.

Keywords BeiDou navigation satellite system (BDS) · Precise point positioning (PPP) · LAMBDA Z -transformation · Uncalibrated phase delay (UPD) · Undifferenced and uncombined

Introduction

Ambiguity resolution (AR) in precise point positioning (PPP) has been demonstrated to take advantage of the integer property of Global Navigation Satellite Systems (GNSS) carrier phase ambiguities through proper handling of satellite and receiver phase delays, leading to reduced

convergence times and improved positioning accuracy (Ge et al. 2008; Laurichesse et al. 2009; Collins et al. 2010; Li et al. 2017; Geng and Shi 2017). With new generations of GNSS space vehicles transmitting three or more frequency signals, GNSS users can possibly make use of observations from additional frequencies. Multi-frequency signals are expected to bring significant improvement to the efficiency and reliability of PPP-AR. In recent years, the study of PPP-AR is changing from using the traditional ionospheric-free (IF) combination to undifferenced and uncombined PPP-AR which has the advantage of lower noise and also reserving the ionospheric parameter (Liu et al. 2016). The undifferenced and uncombined PPP model is also considered as the unified multi-GNSS and multi-frequency positioning model (Liu et al. 2016; Odijk et al. 2016).

One of the keys for successful multi-frequency undifferenced and uncombined PPP-AR is to efficiently and accurately estimate uncalibrated phase delays (UPDs) of multi-frequency observations which can be used to recover

✉ Xiaohong Zhang
xhzhang@sgg.whu.edu.cn

¹ School of Geodesy and Geomatics, Wuhan University, 129 Luoyu Road, Wuhan 430079, Hubei, China
² Collaborative Innovation Center for Geospatial Technology, 129 Luoyu Road, Wuhan 430079, Hubei, China
³ Key Laboratory of Geospace Environment and Geodesy, Ministry of Education, Wuhan University, 129 Luoyu Road, Wuhan 430079, China
⁴ German Research Centre for Geosciences (GFZ), Telegrafenberg, 14473 Potsdam, Germany

the integer property of float ambiguities of each frequency directly. Odijk et al. (2016) built a full-rank GNSS model with ambiguities as integers and then estimate UPDs of each frequency directly. It is wonderful theoretical work and can be easily applied to a multi-frequency and multi-GNSS undifferenced and uncombined PPP network and user positioning. However, Odijk et al. (2017) noted that wide-lane UPDs were more precise than their uncombined counterparts due to its long wavelength. The relative low precision of UPDs was due to high correlation among the multi-frequency ambiguities (Li et al. 2018). This means that estimating the $L1$ frequency UPD directly is influenced by $L2$ and $L3$ frequencies, leading to low precision of the $L1$ UPD. Therefore, instead of estimating UPDs using float ambiguities directly, the method for UPD estimation is usually divided into three steps: first, extract the float ambiguities from the undifferenced and uncombined PPP model; second, estimate the combined UPD of the linear ambiguity combinations; third, recover the UPDs from the combined UPDs. The reason of constructing the linear combinations of ambiguities is that combined ambiguities are less decorrelated, leading to more precise estimation of UPDs (Li et al. 2018). The traditional linear combinations of ambiguities for UPD estimation usually are extra-wide-lane (EWL), wide-lane (WL) and $L1$ combinations which can be characterized by low noise and long wavelengths. However, the selection of EWL, WL and $L1$ combinations is not an optimal strategy for decorrelating the triple-frequency ambiguities maximally (Teunissen 1997, 2002). Therefore, there are two questions: (1) how can we find the maximal decorrelated linear ambiguity combinations to estimate the BDS UPDs; (2) what is the performance of these BDS UPDs in undifferenced and uncombined PPP-AR, compared to the performance of traditional BDS UPDs applied in undifferenced and uncombined PPP-AR?

We start with obtaining float ambiguities using the triple-frequency undifferenced and uncombined PPP model. Then, the method of estimating the BDS UPDs using maximal decorrelated linear ambiguity combinations obtained by the LAMBDA Z -transformation (Teunissen 1995) is proposed. Subsequently, we described the experiment, and analyzed the performance of UPD estimates based on maximal decorrelated linear ambiguity combinations in comparison with the performance of UPD estimates based on traditional linear combinations. The performance of triple-frequency undifferenced and uncombined PPP-AR with two kinds of UPDs also assessed in terms of positioning accuracy and convergence time. Finally, we presented the main conclusions and remarks.

Extraction of original ambiguities

Contrary to Odijk et al. (2016), who estimated the UPDs of each frequency using the full-rank GNSS model, we need to first extract triple-frequency ambiguities. The observation equation for a BDS satellite s observed by receiver r is expressed as follows (Schönemann et al. 2011; Gu et al. 2015; Li et al. 2015):

$$P_{r,n}^s = \rho_r^s + t_r - t^s + \gamma_n \cdot I_{r,1}^s + ZTD + d_{r,n} - d_n^s + \epsilon_{r,n}^s, \quad (1)$$

$$L_{r,n}^s = \rho_r^s + t_r - t^s - \gamma_n \cdot I_{r,1}^s + ZTD + \lambda_n \cdot N_{r,n}^s + \lambda_n \cdot (b_{r,n} - b_n^s) + \xi_{r,n}^s, \quad (2)$$

where $n = 1, 2, 3$ refers to the frequency; ρ_r^s is the geometric distance between the phase centers of satellite and receiver antennas (m); t_r and t^s are the receiver and satellite clock offsets, respectively (m); $d_{r,n}$ and d_n^s denote the frequency-dependent receiver and satellite hardware delays for code observations, respectively (m); $b_{r,n}$ and b_n^s are the uncalibrated phase delays (UPD) for receiver and satellite (cycles). $I_{r,1}^s$ is the slant ionospheric delay on the $L1$ frequency (m); γ_n is the frequency-dependent multiplier factor at frequency n , which can be expressed as $\gamma_n = f_1^2 / f_n^2$ and f is the frequency; ZTD denotes the zenith tropospheric delay (m); λ_n is the wavelength of the phase measurement on the frequency band n (m); $N_{r,n}^s$ is the integer ambiguity (cycles); $\epsilon_{r,n}^s$ and $\xi_{r,n}^s$ are the sum of noise and multipath error for code and carrier phase observations (m). It should be noted that the satellite and receiver antenna phase center offsets (PCOs) and variations (PCVs), relativistic effects, slant hydrostatic troposphere delay, tidal loadings, and phase wind-up (only for carrier phase) have been corrected with the existing models. Note that both the ionospheric delays and pseudorange hardware delay bias of this PPP model are frequency-dependent. This implies that not all parameters can be unbiasedly estimated independently due to rank deficiency, but reparameterization is performed on the basis of the S-system theory (Zhang et al. 2011; Odijk et al. 2016). Therefore, the reparameterized and linearized observation equations can be expressed as:

$$\bar{P}_{r,1}^s = \bar{\rho}_r^s + t_{r,12} + \gamma_1 \cdot \bar{I}_{r,1}^s + m_r^s \cdot zwd_r + \epsilon_{r,1}^s \quad (3)$$

$$\bar{P}_{r,2}^s = \bar{\rho}_r^s + t_{r,12} + \gamma_2 \cdot \bar{I}_{r,1}^s + m_r^s \cdot zwd_r + \epsilon_{r,2}^s \quad (4)$$

$$\bar{P}_{r,3}^s = \bar{\rho}_r^s + t_{r,12} + \gamma_3 \cdot \bar{I}_{r,1}^s + m_r^s \cdot zwd_r + \text{if}b_r^s + \epsilon_{r,3}^s \quad (5)$$

$$\bar{L}_{r,1}^s = \bar{\rho}_r^s + t_{r,12} - \gamma_1 \cdot \bar{I}_{r,1}^s + m_r^s \cdot zwd_r + \bar{N}_{r,1}^s + \xi_{r,1}^s \quad (6)$$

$$\bar{L}_{r,2}^s = \bar{\rho}_r^s + t_{r,12} - \gamma_2 \cdot \bar{I}_{r,1}^s + m_r^s \cdot zwd_r + \bar{N}_{r,2}^s + \xi_{r,2}^s \quad (7)$$

$$\bar{L}_{r,3}^s = \bar{\rho}_r^s + t_{r,12} - \gamma_3 \cdot \bar{I}_{r,1}^s + m_r^s \cdot zw d_r + \bar{N}_{r,3}^s + \xi_{r,3}^s \quad (8)$$

with

$$\begin{cases} \bar{I}_{r,1}^s = I_{r,1}^s - \beta_{12}(\text{DCB}_{r,12} - \text{DCB}^{s,12}) \\ t_{r,12} = t_r + d_{r,IF_{12}} \\ \bar{N}_{r,1}^s = -\gamma_1 \cdot \beta_{12} \cdot (\text{DCB}_{r,12} - \text{DCB}^{s,12}) - d_{r,IF_{12}} + d^{s,IF_{12}} + \lambda_1 \cdot (N_{r,1}^s + b_{r,1} - b_1^s) \\ \bar{N}_{r,2}^s = -\gamma_2 \cdot \beta_{12} \cdot (\text{DCB}_{r,12} - \text{DCB}^{s,12}) - d_{r,IF_{12}} + d^{s,IF_{12}} + \lambda_2 \cdot (N_{r,2}^s + b_{r,2} - b_2^s) \\ \bar{N}_{r,3}^s = -\gamma_3 \cdot \beta_{12} \cdot (\text{DCB}_{r,12} - \text{DCB}^{s,12}) - d_{r,IF_{12}} + d^{s,IF_{12}} + \lambda_3 \cdot (N_{r,3}^s + b_{r,3} - b_3^s) \\ \text{ifb}_r^s = \gamma_3 \cdot \beta_{12} \cdot (\text{DCB}_{r,12} - \text{DCB}^{s,12}) - d_{r,IF_{12}} + d^{s,IF_{12}} + d_{r,3} - d^{s,3} \end{cases} \quad (9)$$

$$\begin{cases} \alpha_{12} = f_1^2 / (f_1^2 - f_2^2) \\ \beta_{12} = -f_2^2 / (f_1^2 - f_2^2) \\ \text{DCB}_{r,12} = d_{r,1} - d_{r,2} \\ \text{DCB}^{s,12} = d^{s,1} - d^{s,2} \\ d_{r,IF_{12}} = \alpha_{12}d_{r,1} + \beta_{12}d_{r,2} \\ d^{s,IF_{12}} = \alpha_{12}d^{s,1} + \beta_{12}d^{s,2} \end{cases}, \quad (10)$$

where \bar{P} and \bar{L} consist of the OMC (observation minus computed) values of pseudorange and carrier phase observations accumulated over each observation epoch, $\bar{\rho}_r^s$ is the geometric distance with satellite orbit and clock offset fixed using the IGS precise product, $t_{r,12}$ refers to the receiver clock error which is based on the B1 and B2 code ionospheric-free combination, $\bar{I}_{r,1}^s$ is the ionospheric delay lumped with receiver and satellite differential code bias on the $L1$ frequency, and ifb_r^s refers to the inter-frequency code bias for each satellite. The reparameterized float ambiguities for each frequency are $\bar{N}_{r,1}^s$, $\bar{N}_{r,2}^s$ and $\bar{N}_{r,3}^s$, henceforth referred to as float ambiguities for simplicity. The symbol $zw d_r$ denotes the wet troposphere delay at zenith with the mapping function m_r^s ; the latter depends on the satellite elevation and receiver location. Further, α_{12} and β_{12} are the frequency factors of ionospheric-free combination, $\text{DCB}^{s,12}$ and $\text{DCB}_{r,12}$ are commonly referred to the differential code bias (DCB) between $P1/P2$ signals for satellite and receiver, respectively, and $d^{s,IF_{12}}$ and $d_{r,IF_{12}}$ are the ionospheric-free pseudorange satellite and receiver hardware delays, respectively.

The proper weighting of the carrier phase and pseudorange observations is an important factor for improving the estimation accuracy. We use an elevation-dependent weighting scheme with a Sine mapping function. Furthermore, we supposed that triple-frequency observables have the same prior noise ($\sigma_1 = \sigma_2 = \sigma_3 = \sigma_0$) (Guo et al. 2016), thus the

stochastic model of undifferenced and uncombined PPP can be expressed as:

$$\Sigma = \begin{bmatrix} \sigma_1^2 & 0 & 0 \\ 0 & \sigma_2^2 & 0 \\ 0 & 0 & \sigma_3^2 \end{bmatrix} = \sigma_0^2 a_0^2 \cdot I, \quad (11)$$

$$a_0 = \begin{cases} 1, & E \geq 30 \\ 1/2 \sin E, & E < 30 \end{cases}, \quad (12)$$

where a_0 is the elevation-dependent weighting factor (Ge et al. 2008), I is the unit matrix, E is the satellite elevation angle, σ_0 is the priori standard deviation for carrier phase and pseudorange observations. The value of σ_0 can be set 0.3 m for pseudorange observations and 0.003 m for phase observations.

Maximal decorrelated linear ambiguity combinations

The ambiguities obtained according to (3)–(8) are known to be highly correlated, which may lead to a relatively low accuracy for UPD estimation. To improve the accuracy of UPD estimation, the traditional idea is to form relatively long wavelength linear combinations of the observations whose combination ambiguities have better precision than the ambiguities. Combinations are commonly referred to as EWL, WL and $L1$ (Gu et al. 2015). Hence, the transformed float ambiguities can be formulated as:

$$\begin{pmatrix} \bar{N}_{r,First}^s \\ \bar{N}_{r,Second}^s \\ \bar{N}_{r,Third}^s \end{pmatrix} = Z_{EWL-WL-L1} \cdot \begin{pmatrix} \bar{N}_{r,1}^s \\ \bar{N}_{r,2}^s \\ \bar{N}_{r,3}^s \end{pmatrix} = \begin{pmatrix} 0 & 1 & -1 \\ 1 & -1 & 0 \\ 1 & 0 & 0 \end{pmatrix} \begin{pmatrix} \bar{N}_{r,1}^s \\ \bar{N}_{r,2}^s \\ \bar{N}_{r,3}^s \end{pmatrix}, \quad (13)$$

where $\bar{N}_{r,1}^s$, $\bar{N}_{r,2}^s$ and $\bar{N}_{r,3}^s$ are the estimated ambiguities of each frequency retrieved from undifferenced and uncombined PPP model; $\bar{N}_{r,First}^s$, $\bar{N}_{r,Second}^s$ and $\bar{N}_{r,Third}^s$ are the EWL,

WL and L1 ambiguities, and $Z_{EWL-WL-L_1}$ is the transformation matrix.

However, as mentioned above, the low precision of ambiguities is mainly due to high correlation between the ambiguities of each frequency. Therefore, we try to find the linear combinations that maximally decorrelate the combination ambiguities. Fortunately, an effective method for constructing maximal decorrelated linear ambiguity combinations is provided by the LAMBDA Z-transformation. The difference between the new combinations constructing by LAMBDA Z-transformation and traditional combinations, lies in the fact that the traditional combinations are selected on the basis of predefined combinations of their carrier frequencies (such as long wavelength and low noise), while the selection by the LAMBDA combinations is based on the complete ambiguity variance–covariance matrix (Teunissen et al. 1997, 2002). It means the combinations searched by the LAMBDA Z-transformation go beyond traditional combinations in its effort to obtain combination ambiguities that are maximally decorrelated and have a better precision. Hence, the decorrelated ambiguities could be formulated as:

$$\begin{pmatrix} \bar{N}_{r,First}^s \\ \bar{N}_{r,Second}^s \\ \bar{N}_{r,Third}^s \end{pmatrix} = Z_{LAMBDA} \cdot \begin{pmatrix} \bar{N}_{r,1}^s \\ \bar{N}_{r,2}^s \\ \bar{N}_{r,3}^s \end{pmatrix} \tag{14}$$

with

$$Q_{\bar{N}_{r,z}^s} = Z_{LAMBDA}^T Q_{\bar{N}_r^s} Z_{LAMBDA} = Z_{LAMBDA}^T L^{-T} D^{-1} L^{-1} Z_{LAMBDA} = \bar{L}^{-T} \bar{D}^{-1} \bar{L}^{-1}, \tag{15}$$

where $\bar{N}_{r,First}^s$, $\bar{N}_{r,second}^s$ and $\bar{N}_{r,Third}^s$ are the first-level, second-level and third-level decorrelated ambiguities, obtained from ambiguities using the LAMBDA Z_{LAMBDA} -transformation matrix; $Q_{\bar{N}_{r,z}^s}$ refers to the triple-frequency decorrelated ambiguity variance–covariance matrix for each receiver–satellite pair; $Q_{\bar{N}_r^s}$ is the original triple-frequency ambiguity variance–covariance matrix for each receiver–satellite pair. As can be seen, Z_{LAMBDA} is the decorrelating transformation matrix which contains maximum decorrelation linear combinations. $Q_{\bar{N}_{r,z}^s}$ is decomposed into the matrix product $\bar{L}^{-T} \bar{D}^{-1} \bar{L}^{-1}$ using LDL-decomposition (De Jonge and Tibertius 1996).

The decorrelated linear combinations obtained from the Z-transformation mainly depend on the stochastic model which decides the ambiguity variance–covariance matrix. The relative priori standard deviation of code and carrier phase observations in this study was chosen as $1/10^2$. Based on the LAMBDA decorrelation results of observations from the 34 stations from CMONOC and APREF, the distributions of three levels of decorrelated linear combinations are shown in Fig. 1. The decorrelated linear combinations,

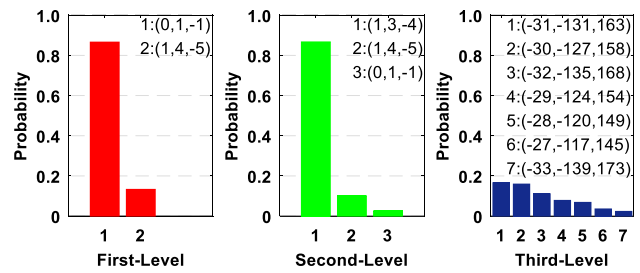


Fig. 1 Distributions of three levels of integer linear combinations based on LAMBDA decorrelation

whose corresponding decorrelated ambiguity had minimum, second and third smallest standard deviation, are defined as first-level, second-level and third-level combinations, respectively. As can be seen, the most frequent combinations were [0, 1, − 1] about 87% probability in first-level, [1, 3, − 4] about 86.6% probability in second-level and [− 31, − 131, 163] about 17% probability in third-level. It is worth noting that the decorrelated coefficients also depend on the changing satellite geometry. However, in this study of specific time and area, we fixed the most probable coefficients as the approximation of the changing coefficients for the purpose of conveniently discussing and comparing maximal decorrelated linear ambiguity combinations with traditional combinations which also fixed coefficients. Therefore,

maximally decorrelated linear combinations were selected according to the probability, and the decorrelated ambiguity as well as Z_{LAMBDA} can be further formulated as:

$$\begin{pmatrix} \bar{N}_{r,First}^s \\ \bar{N}_{r,Second}^s \\ \bar{N}_{r,Third}^s \end{pmatrix} = Z_{LAMBDA} \cdot \begin{pmatrix} \bar{N}_{r,1}^s \\ \bar{N}_{r,2}^s \\ \bar{N}_{r,3}^s \end{pmatrix} = \begin{pmatrix} 0 & 1 & -1 \\ 1 & 3 & -4 \\ -31 & -131 & 163 \end{pmatrix} \cdot \begin{pmatrix} \bar{N}_{r,1}^s \\ \bar{N}_{r,2}^s \\ \bar{N}_{r,3}^s \end{pmatrix}. \tag{16}$$

UPD estimation

After obtaining triple-frequency decorrelated ambiguities according to (14), we first estimated the combined UPDs, which are also known as decorrelated UPDs, instead of UPDs of each frequency directly. The reason was that we could make data preprocessing and quality control more easily. Therefore, to estimate the combined receiver and satellite UPDs, the observation equation can be formulated as (Li and Zhang 2012; Li et al. 2016):

$$R_r^{s,n} = \bar{N}_{r,n}^s - [\bar{N}_{r,n}^s] = -\bar{b}_n^s + \bar{b}_{r,n}^s, \tag{17}$$

where n denotes combinations of first-level, second-level and third-level; $\bar{N}_{r,n}^s$ denotes decorrelated ambiguities in (14); $[\bar{N}_{r,n}^s]$ denotes rounding to the nearest integer of $\bar{N}_{r,n}^s$, which is the sum of the decorrelated ambiguity and the integer part of combined UPDs from receiver r and satellite s ; $\bar{b}_{r,n}$ denotes the fractional part of combined receiver UPD, and \bar{b}_n^s denotes the fractional part of the combined satellite UPD; $R_r^{s,n}$ is the fractional part of combined UPDs from both receiver r and satellite s .

Assuming that m satellites have been tracked in a network of n stations with triple-frequency observations, based on (15), the combined UPDs in one epoch can be further formulated as:

$$\begin{bmatrix} R_1^{1,\text{first}} \\ R_1^{1,\text{second}} \\ R_1^{1,\text{third}} \\ \vdots \\ R_1^{m,\text{first}} \\ R_1^{m,\text{second}} \\ R_1^{m,\text{third}} \\ \vdots \\ R_n^{1,\text{first}} \\ R_n^{1,\text{second}} \\ R_n^{1,\text{third}} \\ \vdots \\ R_n^{m,\text{first}} \\ R_n^{m,\text{second}} \\ R_n^{m,\text{third}} \end{bmatrix} = \begin{bmatrix} -1 & 0 & 0 & \cdots & 0 & 0 & 0 & 1 & 0 & 0 & \cdots & 0 & 0 & 0 \\ 0 & -1 & 0 & \cdots & 0 & 0 & 0 & 0 & 1 & 0 & \cdots & 0 & 0 & 0 \\ 0 & 0 & -1 & \cdots & 0 & 0 & 0 & 0 & 0 & 1 & \cdots & 0 & 0 & 0 \\ \vdots & \vdots & \vdots & \ddots & \vdots & \vdots & \vdots & \vdots & \vdots & \vdots & \ddots & \vdots & \vdots & \vdots \\ 0 & 0 & 0 & \cdots & -1 & 0 & 0 & 1 & 0 & 0 & \cdots & 0 & 0 & 0 \\ 0 & 0 & 0 & \cdots & 0 & -1 & 0 & 0 & 1 & 0 & \cdots & 0 & 0 & 0 \\ 0 & 0 & 0 & \cdots & 0 & 0 & -1 & 0 & 0 & 1 & \cdots & 0 & 0 & 0 \\ \vdots & \vdots & \vdots & \ddots & \vdots & \vdots & \vdots & \vdots & \vdots & \vdots & \ddots & \vdots & \vdots & \vdots \\ -1 & 0 & 0 & \cdots & 0 & 0 & 0 & 0 & 0 & 0 & \cdots & 1 & 0 & 0 \\ 0 & -1 & 0 & \cdots & 0 & 0 & 0 & 0 & 0 & 0 & \cdots & 0 & 1 & 0 \\ 0 & 0 & -1 & \cdots & 0 & 0 & 0 & 0 & 0 & 0 & \cdots & 0 & 0 & 1 \\ \vdots & \vdots & \vdots & \ddots & \vdots & \vdots & \vdots & \vdots & \vdots & \vdots & \ddots & \vdots & \vdots & \vdots \\ 0 & 0 & 0 & \cdots & -1 & 0 & 0 & 0 & 0 & 0 & \cdots & 1 & 0 & 0 \\ 0 & 0 & 0 & \cdots & 0 & -1 & 0 & 0 & 0 & 0 & \cdots & 0 & 1 & 0 \\ 0 & 0 & 0 & \cdots & 0 & 0 & -1 & 0 & 0 & 0 & \cdots & 0 & 0 & 1 \end{bmatrix} \cdot \begin{bmatrix} b_{\text{first}}^1 \\ b_{\text{second}}^1 \\ b_{\text{third}}^1 \\ \vdots \\ b_{\text{first}}^m \\ b_{\text{second}}^m \\ b_{\text{third}}^m \\ b_{1,\text{first}} \\ b_{1,\text{second}} \\ b_{1,\text{third}} \\ \vdots \\ b_{n,\text{first}} \\ b_{n,\text{second}} \\ b_{n,\text{third}} \end{bmatrix} \tag{18}$$

triple-frequency original satellite UPDs for users can be easily recovered as:

$$\begin{bmatrix} b_1^m \\ b_2^m \\ b_3^m \end{bmatrix} = Z_{\text{LAMBDA}}^{-1} \begin{bmatrix} b_{\text{first}}^m \\ b_{\text{second}}^m \\ b_{\text{third}}^m \end{bmatrix}, \tag{20}$$

where b_1^m, b_2^m and b_3^m are the undifferenced satellite UPDs on B1, B2 and B3 frequency, respectively; Z_{LAMBDA}^{-1} is the inversion of Z_{LAMBDA} .

with

$$b_j^s = 0, \quad j = (\text{first,second,third}), \tag{19}$$

where $R_n^{m,\text{first}}, R_n^{m,\text{second}}$ and $R_n^{m,\text{third}}$ are the fractional parts of the first-level, second-level and third-level decorrelated ambiguities, respectively; $b_{\text{first}}^m, b_{\text{second}}^m$ and b_{third}^m are the fractional parts of combined satellite UPDs of the first-level, second-level and third-level, respectively; $b_{n,\text{first}}, b_{n,\text{second}}$ and $b_{n,\text{third}}$ are the fractional parts of combined receiver UPDs of first-level, second-level and third-level, respectively. Equation (19) is the constraint condition to eliminate the rank deficiency of model (18). In (18), the combined UPDs of the satellite for level j , which was observed by most stations, were fixed to zero (Li et al. 2016). The sequential least square estimator was applied to estimate the combined receiver and satellite UPDs. The weights of input ambiguities were set using the inverse of the estimated variance. After obtaining the combined satellite UPDs, the

Experiment analysis and discussions

To validate the advantage of the above-mentioned method, we assessed the performance of the combined satellite UPDs generated by maximal decorrelated linear ambiguity combinations and the traditional combinations (EWL, WL and L1). Three internal precision indicators which are usually used to evaluate the quality of UPDs were analyzed and compared: standard deviation of decorrelated ambiguities, the temporal characteristics of UPDs and the a posteriori residuals of UPD estimates. In addition, to further verify the improvement of undifferenced UPD estimates based on maximal decorrelated linear ambiguity combinations, the performance of BDS undifferenced and uncombined PPP-AR with two kinds of UPD products were conducted. Three groups of PPP solutions were analyzed and compared: triple-frequency PPP float solution (defined as ‘‘Float’’), triple-frequency

PPP-AR using UPDs estimated from the traditional method (defined as “Fix-One”) and triple-frequency PPP-AR using UPDs estimated from the new method (defined as “Fix-Two”). The positioning performance was assessed in terms of convergence time and positioning accuracy. In this study, the horizontal convergence time denoted the time when the horizontal accuracy is better than 10 cm; the vertical convergence time denoted the time when the vertical accuracy was

better than 10 cm. The positioning accuracy was assessed by comparing PPP coordinates with the reference coordinates.

Data collection and PPP resolution strategy

Currently, the BDS visible satellites are mostly confined to the region of 60°S–60°N latitude and 80°E–150°E longitude. To guarantee relatively reliable solutions, we chose the stations where at least five satellites were observed simultaneously at each epoch. Therefore, the BDS ground tracking stations with triple-frequency observation capability were selected in Asia-Pacific regions, as shown in Fig. 2. The 34 stations with 30 s sampling interval observations from CMONOC and APREF were used to estimate UPDs and investigate the performance of PPP-AR. The daily observations from DOY 026–033, 2016, were used in this study. Precise orbit and clock products at intervals of 15 and 5 min, respectively, provided by GFZ were used (Deng et al. 2014). The satellite PCO/PCV corrections are provided by European Space Agency (ESA) were applied for BDS on B1/B2 frequencies (Dilssner et al. 2014). Currently, the PCO/PCV on B3 frequency are still unavailable, the PCO/PCV correction of B2 frequency was used for B3 frequency. More details about BDS PPP processing strategy are summarized in Table 1.

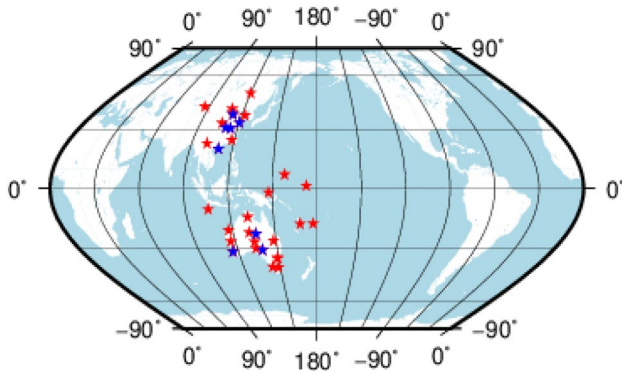


Fig. 2 Distribution of the BDS reference network and user stations. The red stars denote the reference stations for estimating UPDs; the blue stars denote the user stations for investigating the performance of PPP-AR

Table 1 BDS PPP processing strategy

Item	Strategy
Estimator	Sequential least square estimator
Observations	Triple-frequency carrier phase and pseudorange observations
Signal selection	BDS: B1/B2/B3
Sampling rate	30 s
Elevation cutoff	15°
Observations weight	Elevation-dependent weight
Ionospheric delay	Estimated as white noise process
Tropospheric delay	Dry component: corrected with GPT model (Boehm et al. 2007) Wet component: estimated as random-walk process, GMF mapping function
Receiver clock	Estimated as white noise
Station displacement	Corrected by IERS Convention 2010, including Solid Earth tide pole tide and ocean tide loading (Petit and Luzum 2010)
Satellite PCO/PCV	Corrected using ESA values
Receiver PCO/PCV	Corrected using GPS values from ESA
Phase wind-up effect	Corrected (Wu et al. 1993)
Relativistic effect	Applied
Station coordinate	Static PPP: estimated as constants
Phase ambiguities	Float: constant for each continuous arc, without ambiguity resolution Fix-one: ambiguity resolution with UPDs based on traditional method Fix-two: ambiguity resolution with UPDs based on new method

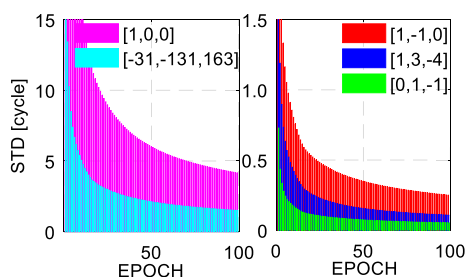


Fig. 3 Standard deviation of combined ambiguities with the first 100-epoch observations on DOY 026, 2016. The new combinations $[0, 1, -1]$, $[1, 3, -4]$ and $[-31, -131, 163]$ are from the LAMBDA Z-transformation, whereas $[0, 1, -1]$, $[1, -1, 0]$ and $[1, 0, 0]$ are the traditional EWL, WL and L1 combinations

Evaluating the characteristics and performance of the combined UPDs

As introduced above, the combined UPDs are estimated from the combined ambiguities which are constructed by the new or traditional linear combinations. Therefore, the precision of the combined ambiguities is essential for undifferenced UPD estimates. Figure 3 shows the standard deviation (STD) of combined ambiguities for the first 100-epoch observations. As can be seen, the linear combination with the smallest estimated standard deviation of combined ambiguities is $[0, 1, -1]$. The linear combination which has the second smallest estimated standard deviation of combined ambiguities is $[1, 3, -4]$ generated from the LAMBDA Z-transformation instead of traditional WL combination in (11). Although the third-level linear combination of $[-31, -131, 163]$ generated from the LAMBDA Z-transformation

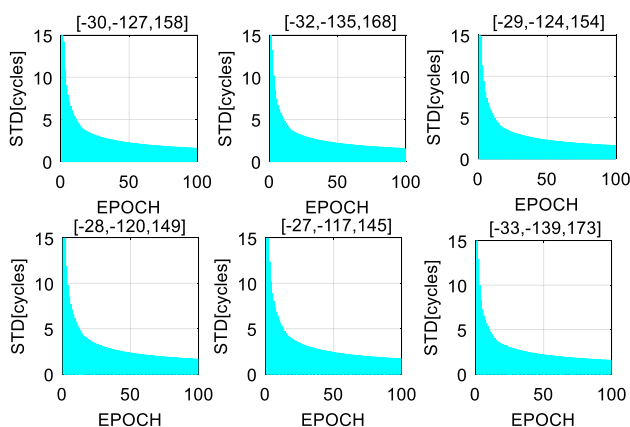


Fig. 4 Standard deviation of combined ambiguities using the first 100-epoch observations on DOY 026, 2016 $[-30, -127, 158]$, $[-32, -135, 168]$, $[-29, -124, 154]$, $[-28, -120, 149]$, $[-27, -117, 145]$ and $[-33, -139, 173]$ combinations were the third-level combinations resulting from the LAMBDA Z-transformation

had a relatively big estimated standard deviation of combined ambiguities, it still had a smaller estimated standard deviation of combined ambiguities than the L1 combination in (11). In addition, it is worth noting that the weak structure of the receiver–satellite spatial geometry for current BDS observations leads to a large value of the third-level combination of $[-31, -131, 163]$. Although the large value of this linear combination could lead to higher noise, it still had better precision than the linear combination of $[1, 0, 0]$ which was highly correlated. In addition to study the ambiguities of the most probable $[-31, -131, 163]$ combination, the standard deviation of the combined ambiguities which used the other six third-level combinations is also showed in Fig. 4. As can be seen, although the seven groups of third-level combination were different in coefficients and probability of occurrence, the precision of these combined ambiguities was almost same.

To compare the temporal stability and decide the update time interval, the time series of two kinds of the combined UPDs are depicted for each epoch on DOY 026, 2016 in

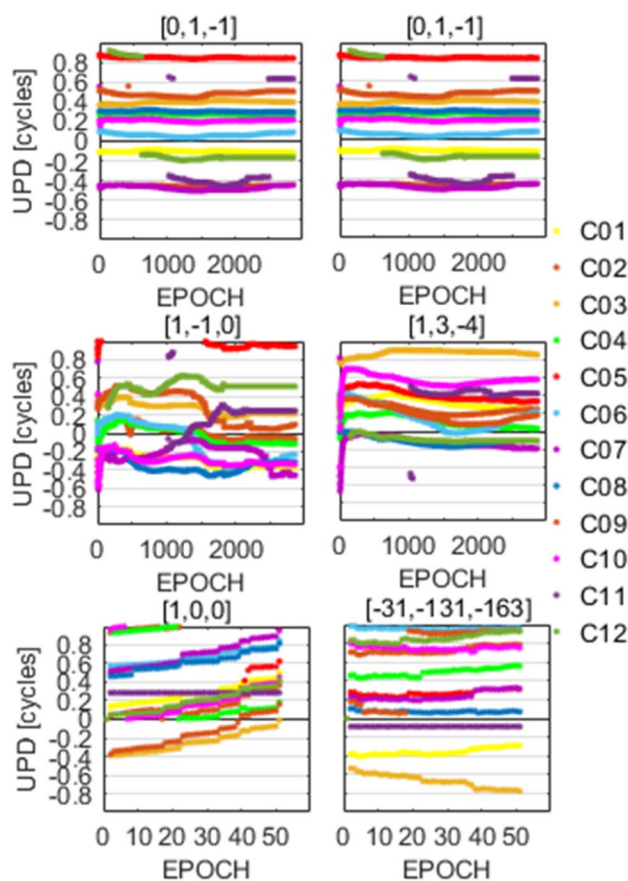


Fig. 5 Time series of combined UPDs for each epoch of DOY 026, 2016. The three combinations $[0, 1, -1]$, $[1, 3, -4]$ and $[-31, -131, 163]$ were obtained from LAMBDA Z-transformation (right panel), while the combinations $[0, 1, -1]$, $[1, -1, 0]$ and $[1, 0, 0]$ were from traditional EWL WL and L1 (left panel)

Fig. 5. In this study, the update time interval of UPD products denotes the time it takes for the variation of UPD to be more than 0.1 cycles. The left panels show the three groups of combined UPDs estimated from traditional ambiguity combinations and the right panels show the three groups of combined UPDs estimated from maximal decorrelated linear ambiguity combinations. As can be seen, the $[0, 1, -1]$ combination UPD which could be generated from both traditional EWL and new maximally decorrelated combinations, is the most stable and its daily averaged variation is about 0.062 cycles. Hence, the $[0, 1, -1]$ combination UPD can be estimated on a daily basis with an update time interval of 1 day. The reason why the EWL UPDs are so stable is that the EWL ambiguities not only characterize a long wavelength but also do not depend on the geometric range and some atmosphere delay errors. Compared to the $[1, -1, 0]$ combination UPD, the $[1, 3, -4]$ combination UPD is more stable and its averaged variation is about 0.082 cycles within 12 h. Hence, the $[1, 3, -4]$ combination UPD can be updated with a time interval of 12 h. It is noted that the $[1, 3, -4]$ combination ambiguities have the same characteristics as EWL ambiguities, but the relative short wavelength of the $[1, 3, -4]$ combination ambiguities is more easily impacted by measurement noise and multipath effects, which leads to the relative instability of UPDs. Although the $[1, 0, 0]$ UPD and the $[-31, -131, 163]$ combination UPD were not stable, as expected, the averaged variation of the $[-31, -131, 163]$ combination UPD could still reach up to 0.095 cycles for the time interval of ten epochs. Therefore, the $[-31, -131, 163]$ combination UPD can be considered as high quality in a time interval of 5 min. The $[1, 0, 0]$ and $[-31, -131, 163]$ combination UPDs are not stable because they are impacted by geometric range as well as atmosphere delay errors. However, compared to the $[1, 0, 0]$ ambiguity, the $[-31, -131, 163]$ combination ambiguity can generate more stable UPDs because it is more decorrelated and also has longer wavelength. In addition to analyzing the most probable $[-31, -131, 163]$ combination, the time series of UPDs generated by the other Third-Level combinations are showed in Fig. 6. It can be seen that the stability of the seven groups of UPDs of third-level combination shows no significant difference.

The a posteriori residuals of the UPD estimation are usually calculated by evaluating the internal precision of UPD estimates. Distributions of residuals of combined UPD estimates based on the traditional combinations and maximal decorrelated linear ambiguity combinations on DOY 026, 2016 are demonstrated in Fig. 7. The best performance of the internal precision is seen for the $[0, 1, -1]$ combination UPD, in which case the root-mean-square (RMS) of residuals is about 0.033 cycles, and almost 100% residuals were within 0.2 cycles. Compared to the performance of the $[1, -1, 0]$ combination UPD estimates, the performance of the

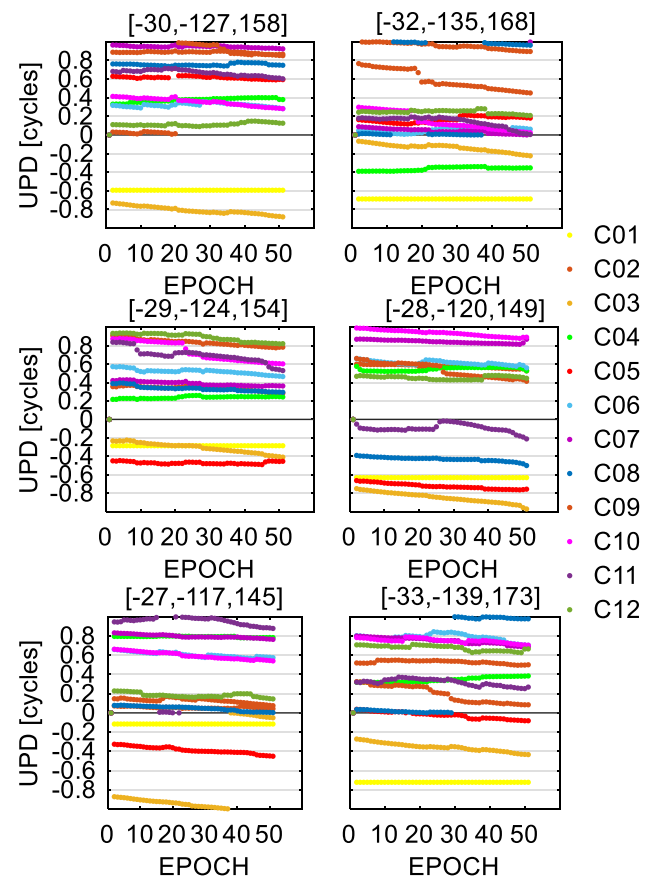


Fig. 6 Time series of combined UPDs for each epoch of DOY 026, 2016. $[-30, -127, 158]$, $[-32, -135, 168]$, $[-29, -124, 154]$, $[-28, -120, 149]$, $[-27, -117, 145]$ and $[-33, -139, 173]$ combinations were obtained from LAMBDA Z-transformation

$[1, 3, -4]$ combination UPD estimates is better. It is clear that the RMS of the residuals of the $[1, -1, 0]$ combination UPD estimates is 0.089 cycles, while the RMS of the residuals of the $[1, 3, -4]$ combination UPD estimates is only 0.053 cycles, which is an improvement of 40.4%. The performance of the $[-31, -131, 163]$ combination UPD estimates is slightly better than that of the $[1, 0, 0]$ combination UPD estimates, having an improvement of 12.6% in terms of RMS of residuals. Therefore, the statistical results indicate that the internal precision of the combined satellite UPDs estimated from the new ambiguity decorrelated combinations is better than that estimated from EWL, WL and $L1$ combinations.

Performance of undifferenced UPDs tested in PPP-AR

After the undifferenced UPDs were recovered from the combined UPDs in (20), undifferenced and uncombined PPP-AR can be performed for verifying the improvement of the UPD

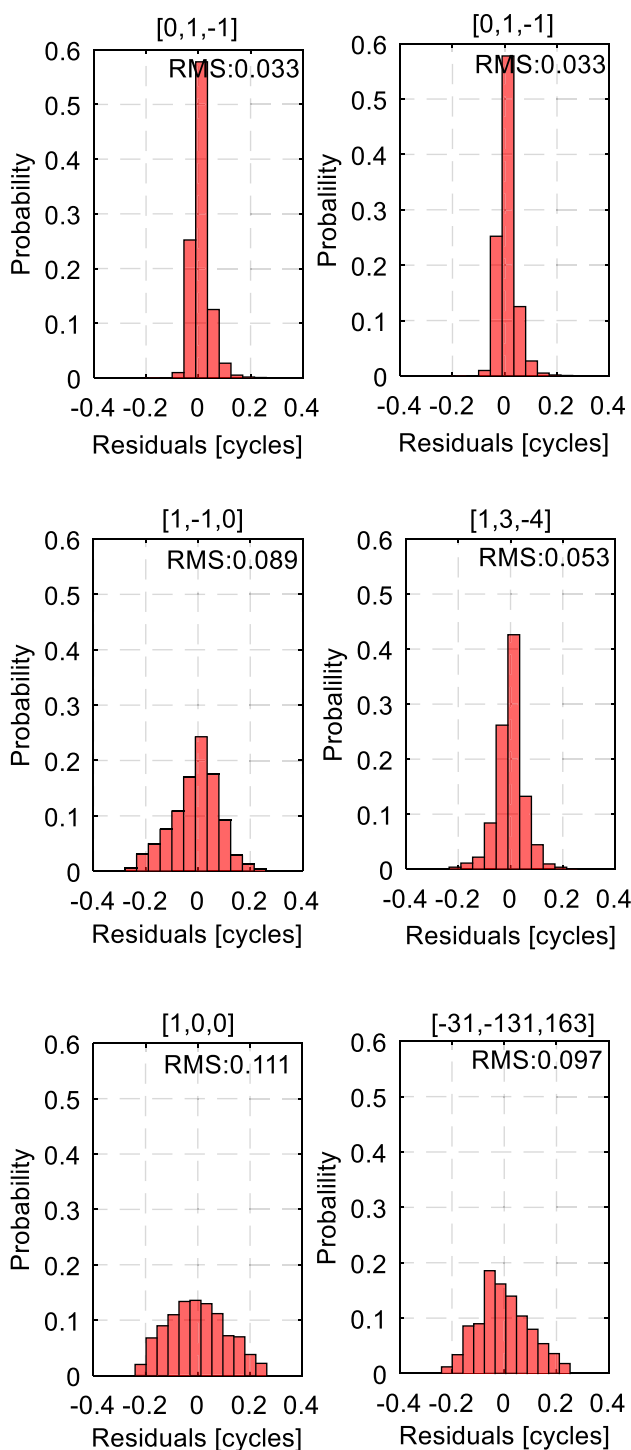


Fig. 7 Distribution of residuals of the combined UPD estimates based on the traditional combinations (left panel) and maximal decorrelated linear ambiguity combinations (right panel) on DOY 026, 2016

estimates using maximal decorrelated linear ambiguity combinations. Figure 8 shows the averaged positioning error for PPP solutions with the first 200-epoch observations for all

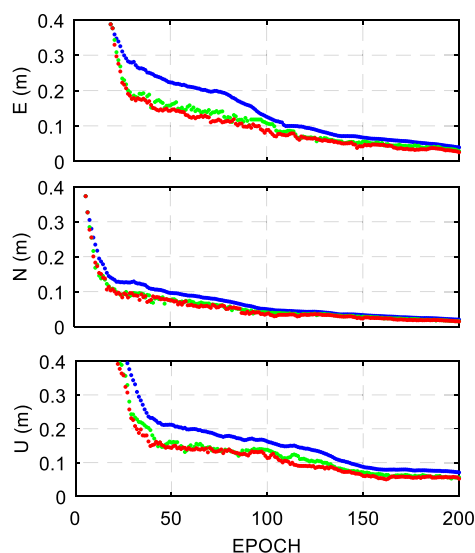


Fig. 8 Averaged positioning error in the east (top), north (middle), up (bottom) components for three groups of PPP solutions with the first 200-epoch observations for all test stations on days 026–033, 2016. The Float, Fix-One, and Fix-Two are presented as blue, green, and red, respectively

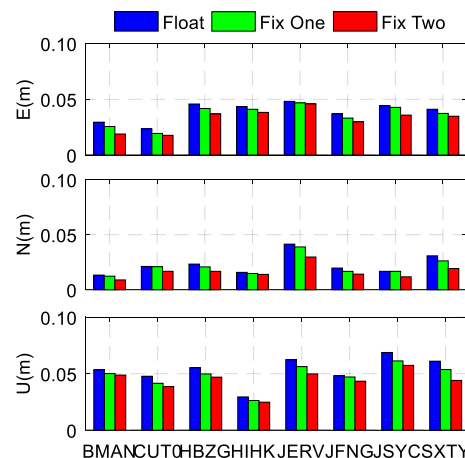


Fig. 9 Averaged positioning error in the east (top), north (middle), up (bottom) components for three groups of PPP solutions with 3 h observation for each test stations on days 026–033, 2016. Float, Fix-One, and Fix-Tow are presented in blue, green, and red, respectively

test stations on DOY 026–033, 2016. Three groups of PPP solutions for “Float”, “Fix-One” and “Fix-Two” are shown in blue, green and red, respectively. As can be seen, the PPP fixed solutions showed an obvious better performance than the PPP float solution in terms of positioning accuracy and convergence time. For Fix-Two, it took 103 epochs to achieve a horizontal accuracy of better than 10 cm and 121 epochs to achieve a vertical accuracy of better than 10 cm. Compared with Fix-One, Fix-Two reduced the convergence time by 8.9% and 12.3% in horizontal and vertical direction.

Table 2 Mean and STD of positioning error with 3 h observation for all test stations (unit: cm)

Direction	Mean			STD		
	Float	Fix-One	Fix-Two	Float	Fix-One	Fix-Two
E	3.9	3.6	3.2	2.6	2.4	2.1
N	2.5	2.2	2.0	2.3	2.2	2.0
U	5.3	4.8	4.4	4.4	4.1	3.9

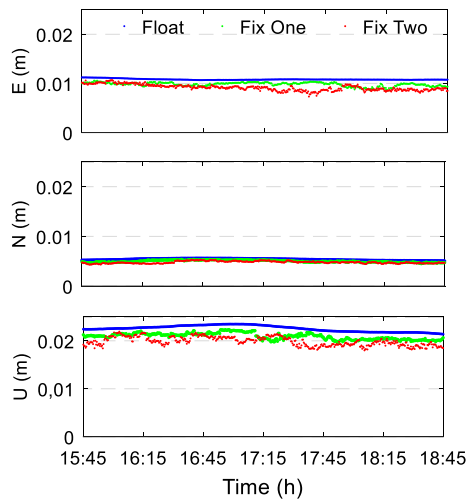


Fig. 10 Averaged positioning error in the east (top), north (middle), up (bottom) components for three groups of PPP solutions with observations between 15:45 and 18:45 for all test stations on day 026–033, 2016. The Float, Fix-One, and Fix-two are shown in blue, green, and red, respective

Table 3 STD and the maximum difference of positioning bias for the three group of PPP solution with observations between 15:45 and 18:45 for all test stations (unit: cm)

Direction	STD			Maximum	
	Float	Fix-One	Fix-Two	Diff-1	Diff-2
E	0.01	0.04	0.04	0.4	0.3
N	0.01	0.02	0.02	0.1	0.1
U	0.06	0.07	0.09	0.4	0.3

Compared to Float, the Fix-Two reduced convergence time by 14.2% and 20.3% in horizontal and vertical direction.

For the purpose of testing the performance of the undifferenced UPDs applied in PPP-AR during other session, the averaged positioning accuracy information of 3 h static PPP-AR for each station over all test days is given in Fig. 9. Table 2 also presents the mean and the STD of positioning error for the session data, which can evaluate external accuracy and internal precision, respectively. It can be seen that the PPP solutions with 3 h observation could achieve an accuracy of less than 5 cm in horizontal directions and

10 cm in vertical directions, respectively. The highest positioning accuracy was achieved by the Fix-Two with the averaged accuracy of 3.2, 2.0 and 4.4 cm in the east, north and up directions, respectively. It improved the positioning accuracy by 18, 20 and 17% compared to Float and 11.1, 9.1 and 8.3% compared to Fix-One in the east, north and up directions, respectively.

Figure 10 shows averaged positioning error for all test stations of the three groups of the PPP solutions between 15:45 and 18:45 on days 026–033, 2016. Table 3 presents the STD of positioning error and the maximum difference of positioning error between Fix-Two and Float (defined as Diff-1) as well as Fix-Two and Fix-One (defined as Diff-2) for the session data. One can see that currently the three-frequency BDS static PPP with about a dozen-hour observation can achieve an accuracy of 0.8–1.2 cm in east, 0.4–0.6 cm in north and 1.5–2.5 cm in up directions, respectively. As expected, the ambiguity-fixed PPP is obviously superior to the float PPP solution. Fix-Two showed the best performance in terms of positioning accuracy. The maximum difference of the positioning error between fixed solutions and float solution reached up to 0.4 cm in east, 0.1 cm in north and 0.4 cm in up directions, respectively.

It was noted that the float solution was more stable than the ambiguity-fixed solutions. The reason we think is that the estimates of UPDs are impacted by some residual atmospheric delays which are time-varying, such as high-order ionospheric delay. However, the standard deviation of each solution is at the sub-millimeter level based on the statistics in Table 3. Therefore, the difference in stability between float solutions and fixed solutions could be ignored in practical applications.

As discussed above, the third-level maximal decorrelated linear ambiguity combinations have seven different sets of coefficients; however, Fix Two only used UPDs generated by the most probable coefficient. Therefore, it is necessary to evaluate the performance of Fix Two when using the UPDs generated by the other maximal decorrelated linear ambiguity combinations. The positioning results of stations HBZG and HHHK are shown in Fig. 11 where ‘1’ denotes Fix Two using UPDs generated by the most probable coefficient, and ‘2’-‘6’ denote Fix Two using UPDs generated by the other maximal decorrelated linear ambiguity combinations. As can be seen, the performance of PPP-AR with the seven

- 1:Fix Two
- 2:Fix Two (-30,-127,158)
- 3:Fix Two (-32,-135,168)
- 4:Fix Two (-29,-124,154)
- 5:Fix Two (-28,-120,149)
- 6:Fix Two (-27,-117,145)
- 7:Fix Two (-33,-139,173)

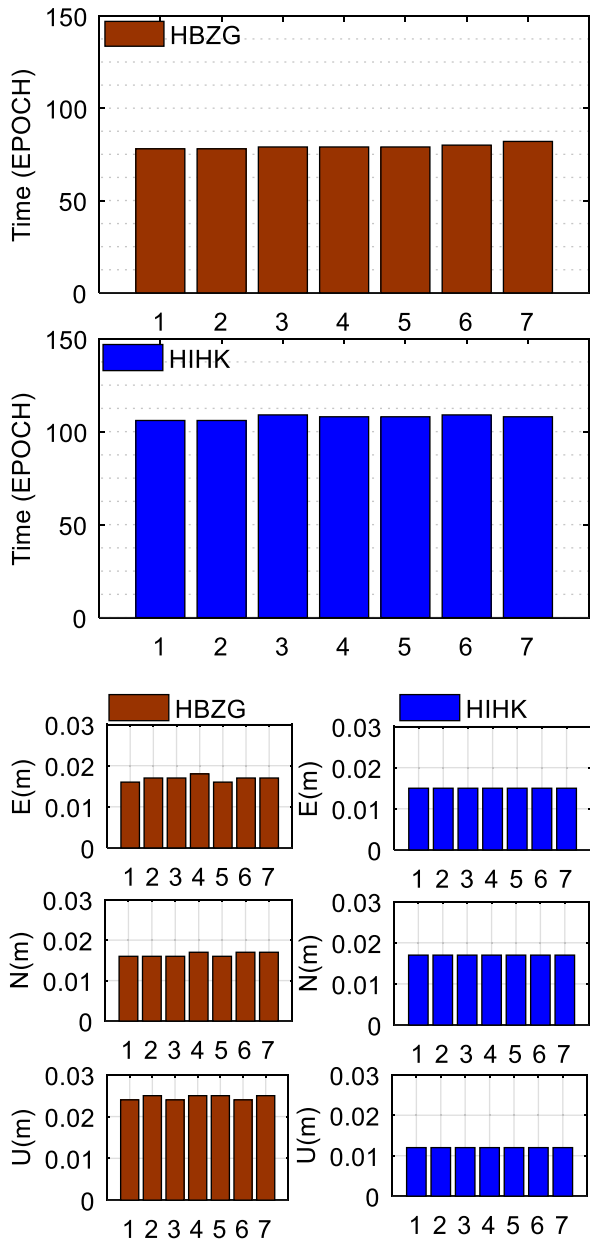


Fig. 11 Convergence time and daily positioning error of seven groups of PPP-AR solutions for stations HBZG and HCHK on DOY 026, 2016

groups of UPDs has no significant difference in terms of convergence time and positioning accuracy. This could be contributed to almost the same precision of the seven groups of combined ambiguities as well as the similar quality of the seven groups of UPDs which was shown above. Therefore, it

is reasonable to fix the most probable coefficients as approximation of the changing coefficients.

Conclusions and remarks

We studied the method of estimating multi-frequency undifferenced satellite UPD using maximal decorrelated linear ambiguity combinations. The traditional EWL, WL and L1 combinations are not optimal for triple-frequency BDS UPD estimation. Maximal decorrelated linear ambiguity combinations obtained from the LAMBDA Z-transformation are more applicable than traditional combinations for BDS UPD estimation. The reason is that the triple-frequency undifferenced ambiguities, which are usually high related, could be maximally decorrelated by the new combinations.

We verified the method using 34 stations with BDS triple-frequency observations from CMONOC and APREF in Asia-Pacific regions. The results showed the internal precision of the combined UPD estimates based on maximal decorrelated linear ambiguity combinations is better than that based on traditional combinations. In addition, PPP-AR using UPDs based on the new combinations shows improvement in positioning accuracy and convergence time, compared to PPP-AR using UPDs based on traditional combinations. The statistical results demonstrate that an averaged positioning error of 3.2, 2.0 and 4.4 cm in the east, north and up directions, respectively, can be obtained by triple-frequency PPP-AR using UPDs based on the new combinations over 3 h observation. It improved the positioning accuracy by 11.1, 9.1 and 8.3% compared with PPP-AR with UPDs based on traditional combinations, and by 18, 20 and 17% compared with float PPP in the east, north and up directions, respectively. Furthermore, with about 15 h of observation, an averaged positioning accuracy of 1.0, 0.5 and 2.0 cm in the east, north and up directions, respectively, can be achieved by PPP-AR using UPDs based on the new combinations. PPP-AR using UPDs based on the new combinations reduced the average convergence time by 14.2% and 20.3% in horizontal and vertical directions compared with float PPP, and 8.9% and 12.3% in horizontal and vertical directions compared with PPP-AR using UPDs based on traditional combinations.

Acknowledgements The authors were grateful to the many individuals and organizations who contributed to the International GNSS Service. We also gratefully acknowledged the use of Generic Mapping Tool (GMT) software. This research was funded by National Science Fund for Distinguished Young Scholars (Grant no. 41825009), the National Key Research and Development Program of China (nos. 2016YFB0501803, 2017YFB0503402), National Natural Science Foundation of China (no. 41774034), and the project of Wuhan Science and Technology Bureau (no. 2018010401011270).

References

- Boehm J, Heinkelmann R, Schuh H (2007) Short note: a global model of pressure and temperature for geodetic applications. *J Geod* 81(10):679–683
- Collins P, Bisnath S, Lahaye F, Héroux P (2010) Undifferenced GPS ambiguity resolution using the decoupled clock model and ambiguity datum fixing. *Navigation* 57(2):123–135
- De Jonge P, Tiberius C (1996) The lambda method for integer ambiguity estimation: implementation aspects. Technical Report LGR Series, No. 12
- Deng Z, Zhao Q, Springer T, Prange L, Uhlemann M (2014) Orbit and clock determination-BeiDou. In: Proceedings of IGS workshop 2014, June 23–27, 2014, Pasadena, USA
- Dilssner F, Springer T, Schönemann E, Enderle W (2014) Estimation of satellite Antenna Phase Center corrections for BeiDou. In: Proceedings of IGS workshop 2014, June 23–27, 2014, Pasadena, USA
- Ge M, Gendt G, Rothacher M, Shi C, Liu J (2008) Resolution of GPS carrier-phase ambiguities in precise point positioning (PPP) with daily observations. *J Geod* 82(7):389–399
- Geng J, Shi C (2017) Rapid initialization of real-time PPP by resolving undifferenced GPS and GLONASS ambiguities simultaneously. *J Geod* 91(4):361–374
- Gu S, Lou Y, Shi C, Liu J (2015) Beidou phase bias estimation and its application in precise point positioning with triple-frequency observable. *J Geod* 89(10):979–992
- Guo F, Zhang XH, Wang JL, Ren XD (2016) Modeling and assessment of triple-frequency BDS precise point positioning. *J Geod* 90(11):1223–1235
- Laurichesse D, Mercier F, Berthias JP, Broca P, Cerri L (2009) Integer ambiguity resolution on undifferenced GPS phase measurements and its application to PPP and satellite precise orbit determination. *Navigation* 56(2):135–149
- Li X, Zhang X (2012) Improving the estimation of uncalibrated fractional phase offsets for PPP ambiguity resolution. *J Navig* 65(3):513–529
- Li X, Ge M, Dai X, Ren X, Fritsche M, Wickert J, Schuh H (2015) Accuracy and reliability of multi-GNSS real-time precise positioning: GPS, GLONASS, BeiDou, and Galileo. *J Geod* 89(6):607–635
- Li P, Zhang X, Ren X, Zuo X, Pan Y (2016) Generating gps satellite fractional cycle bias for ambiguity-fixed precise point positioning. *GPS Solut* 20(4):771–782
- Li X, Li X, Yuan Y, Zhang K, Zhang X, Wickert J (2017) Multi-GNSS phase delay estimation and PPP ambiguity resolution: GPS, BDS, GLONASS, Galileo. *J Geod* 92(6):579–608
- Li P, Zhang X, Ge M, Schuh H (2018) Three-frequency BDS precise point positioning ambiguity resolution based on raw observables. *J Geod* 5:1–13
- Liu T, Yuan Y, Zhang B, Wang N, Tan B, Chen Y (2016) Multi-GNSS precise point positioning (MGPPP) using raw observations. *J Geod* 91(3):253–268
- Odijk D, Zhang B, Khodabandeh A, Odolinski R, Teunissen PJG (2016) On the estimability of parameters in undifferenced, uncombined GNSS network and PPP-RTK user models by means of S-system theory. *J Geod* 90(1):15–44
- Odijk D, Khodabandeh A, Nadarajah N, Choudhury M, Zhang B, Li W, Teunissen PJG (2017) PPP-RTK by means of S-system theory: Australian network and user demonstration. *J Spat Sci* 62(1):3–27
- Petit G, Luzum B (2010) IERS Conventions 2010 (IERS Technical Note No. 36). Verlag des Bundesamts für Kartographie und Geodäsie, Frankfurt am Main, p 179
- Schönemann E, Becker M, Springer T (2011) A new approach for GNSS analysis in a multi-GNSS and multi-signal environment. *J Geod Sci* 1(3):204–214
- Teunissen PJG (1995) The least-squares ambiguity decorrelation adjustment a method for fast GPS integer ambiguity estimation. *J Geod* 70(1–2):65–82
- Teunissen PJG (1997) On the GPS widelane and its decorrelating property. *J Geod* 71(9):577–587
- Teunissen PJG, Joosten P, Tiberius C (2002) A comparison of TCAR, CIR and LAMBDA GNSS ambiguity resolution. In: Proceedings of ION GPS 2002, Institute of Navigation, Portland, OR, September 24–27, pp 2799–2808
- Wu J, Wu S, Hajj G, Bertiger W, Lichten S (1993) Effects of antenna orientation on GPS carrier phase. *Manuscr Geod* 18:91–98
- Zhang B, Teunissen PJG, Odijk D (2011) A novel undifferenced PPP-RTK concept. *J Navig* 64(S1):S180–S191

Publisher's Note Springer Nature remains neutral with regard to jurisdictional claims in published maps and institutional affiliations.



Gen Liu is currently a Ph.D. candidate at the School of Geodesy and Geomatics, Wuhan University, China. He obtained his B.Sc. and Master degrees in 2013 and 2016, respectively. His current research focuses on multi-frequency precise point positioning ambiguity resolution.



Xiaohong Zhang is currently a professor at the Wuhan University. He obtained his B.Sc., Master, and Ph.D. degrees with distinction in Geodesy and Engineering Surveying at the School of Geodesy and Geomatics in Wuhan University in 1997, 1999 and 2002. His main research interests include Precise Point Positioning and GNSS/INS.



Pan Li is currently a scientist at the German Research Centre for Geosciences (GFZ). He obtained his Ph. D. degree at the Wuhan University in 2016. His current research mainly focuses on multi-frequency and multi-system GNSS data processing, particularly PPP ambiguity resolution.